Landslides:Evaluation and Stabilization, W.A. Lacerda, M. Ehrlich, S.A.B. Fontura & A.S.F. Sayão (eds)

v. 1, p. 69-78

Landslide susceptibility from topography in Guatemala

J.A. Coe, J.W. Godt, R.L. Baum, R.C. Bucknam & J.A. Michael
U.S. Geological Survey, MS 966, Denver Federal Center, Denver, Colorado U.S.A. 80225

ABSTRACT: We present a landslide susceptibility map of a 980 sq. km area in east-central Guatemala that was impacted by Hurricane Mitch in 1998. Susceptibility was based on a ratio between topographic parameters at Mitch landslide DEM cells to those of a random sampling of DEM cells within the study area. Ratios for four topographic parameters (elevation, slope angle, planform curvature, and aspect) were calculated, but we found that two of these, a combination of elevation (a proxy for rainfall) and slope angle, best portrayed landslide susceptibility. The map produced from these two parameters includes 80 percent of landslides initiated by Mitch within susceptible zones, and classifies 71 percent of the study area as having no preferred susceptibility. Seventy–five percent of pre-Mitch landslides, and 90 percent of post-Mitch landslides, also fall within susceptible zones. Similar results probably could be expected for other geographic areas where there is a correlation between elevation and rainfall accumulation.

1 INTRODUCTION

Landslide susceptibility can be mapped using a number of different methods depending on the data available (e.g., Soeters & van Westen 1996, Guzzetti et al. 1999, Savage et al., this volume). Numerous recent studies use various statistical techniques and incorporate many (5 or more) parameters such as topography, geology, hydrology, and land-use in Geographic Information Systems (GIS) to derive landslide susceptibility (e.g., Chung & Fabbri 1999, Lineback et al. 2001, Santacana et al. 2003). Physically-based methods rely on physical properties of hillslope materials and topographic information from a digital elevation model (DEM) in slope-stability models (e.g., Montgomery & Dietrich 1994, Jibson et al. 2000, Savage et al. 2003). In many parts of the world however, the abundance of data such as that described above is not available, but the need for landslide susceptibility maps is great (e.g., Pallàs et al., in press). A question asked is: Can reliable susceptibility maps be produced from limited data? Fabbri et al. (2003) suggested that this is not only possible, but, in at least one example, possibly more accurate. They outlined seven "myths" associated with GIS modeling of landslide hazard. Two of these myths were: 1) the more data layers we have, the better the prediction, and 2) the only thing we have is a DEM from satellite or aerial imagery or a topographic base-map; therefore we cannot make a prediction map. They evaluated the effectiveness of a landslide susceptibility map made using 6 data layers (including geology, surficial materials, land use, slope, elevation, and aspect) vs. one made using 3 data layers (slope, elevation, and aspect) and found that the 3 data layers (derived exclusively from a DEM) provided better results, seemingly indicating that topography was the dominant control in determining landslide location.

Some of our work at the U.S. Geological Survey (USGS) involves responding to landslide disasters. One of these disasters was caused by Hurricane Mitch in Guatemala in 1998 (Bucknam et al. 2001). As part of our work following Hurricane Mitch we produced a landslide susceptibility map using two types of data, a landslide inventory map, and a DEM. Because of a lack of data, we were forced to confront the two "myths" given above. This paper grew out of this confrontation. In what follows, we describe our effort to map relative landslide susceptibility using inventory and DEM data. We estimate relative landslide susceptibility based on a comparison (a ratio) of topographic parameters at landslide DEM cells to the same parameters at a random sampling of the entire population of DEM cells. Although ratio methods are not new in landslide susceptibility mapping, to our knowledge, our approach differs from previous work in the way we combine parameters using a moving-count circle approach (Savage et al. 2001) to produce a susceptibility map for a 980 km^2 study area in east-central Guatemala that was impacted by Hurricane Mitch.

2 THE GUATEMALA STUDY AREA

The Guatemala study area encompasses two 1:50,000-scale topographic maps (Fig. 1) and is be-

tween the Motagua and Polochic rivers in the Sierra de las Minas mountain range in east-central Guatemala. The area lies between the Motagua and Polochic faults, two of the largest strike-slip faults in Central America (Bonis et al. 1970, Espinosa 1976, Tobisch 1986). Hillslopes in the study area tend to be steep and difficult to access from the ground or air. Elevations range from just above sea level to 3,000 m. Climate zones in the area range from arid at lower elevations to montane rain forest at higher elevations. Large-scale geologic mapping in the area is incomplete (e.g., Newcomb 1978), and physical-property data are not available for hillslope materials.

The area was impacted by Hurricane Mitch between October 27 and November 1, 1998 (Lott et al. 1999, Bucknam et al. 2001). Within the area, two rain gages indicated that cumulative rainfall during this period ranged from 125 mm at an elevation of 250 m, to 275 mm at an elevation of 1780 m (Bucknam et al. 2001). As part of the U.S. Agency for International Development (USAID) Hurricane Mitch Reconstruction Program, the USGS, in collaboration with the Instituto Nacional de Sismología, Vulcanología, Meteorología e Hidrología (INSIVUMEH), conducted a comprehensive inventory of landslides triggered by Mitch within a 10,000 km^2 area adjacent to the Motagua and Polochic rivers. This mapping effort established that about 2,950 landslides occurred within the 980 km^2 study area during Mitch (Fig. 1), with most of the landslides mobilizing as debris flows (Bucknam et al. 2001). Many of the debris flows coalesced in drainages and flowed great distances (up to about 15 km) to alluvial fans at the base of the mountain range. Several of the debris flows damaged bridges and houses, and Highway CA9 in the Motagua Valley was impacted and closed.

In addition to landslides triggered by Hurricane Mitch, pre-Mitch and post-Mitch landslides (Fig. 2) were also mapped in the study area (Bucknam et al. 2001). We use the Mitch landslides to develop the susceptibility map and the pre- and post-Mitch landslides to evaluate the effectiveness of the map for landslide prediction during more commonly occurring storms.

As part of the landslide mapping effort, landslide-initiation locations (the upslope end of each mapped landslide, i.e., the head scarp) were identified and digitized (as points), and a 10-m resolution DEM was generated from the 20-m elevation contours on the two topographic maps (Bucknam et al. 2001).

3 DESCRIPTION OF METHODOLOGY

To determine the topographic parameters that contribute to landslide susceptibility, we used the 10-m DEM and the ArcInfo GIS to determine elevation, slope angle, topographic planform curvature, and aspect (direction of slope) at each landslide-initiation location. We generated frequency distributions (as percentage of total) $f(p_i)$, for each of these parameters, p_i, throughout the map area, and for landslide-initiation locations with respect to each parameter, $fl(p_i)$. A ratio, $R(p_i)$, between the two distributions determines the relative landslide susceptibility for the i^{th} parameter and can be used to map relative landslide susceptibility:

$$R(p_i) = fl(p_i) / f(p_i) \quad (1).$$

Values of $R(p_i)$ greater than one indicate preferred susceptibility (see Wieczorek et al. 1988, Coe & Godt 2001, and Lee et al. 2002, for other examples of this approach). The approach outlined in equation 1 can be extended to *n*-dimensional (multi-parameter) frequency distributions $fl(p_1, p_2,\ldots, p_n)$ and $f(p_1, p_2,\ldots, p_n)$ to create a landslide susceptibility map. For the Guatemala study area, we found that slope angle and elevation best portrayed landslide susceptibility during Hurricane Mitch. In the paragraphs that follow, we describe the analysis of these two parameters and the resulting susceptibility map based on a two-parameter frequency distribution.

3.1 Analysis of Elevation

About 96 percent of the landslides initiated at elevations between 500 and 2500 m assuming initiation occurred at the topographically highest point on each landslide (Fig. 3). When landslide frequency is tabulated in 100 m elevation increments (bins), the highest percentage of landslides (about 12 percent of the total) initiated between 2000 and 2100 m. The entire population of elevations at 10-m DEM cells in the two quadrangles ranged from 1 m to about 2990 m (Fig. 3). The highest percentage of these elevations (about 11 percent of the total) is between 200 m and 300 m. The ratio $R(elevation)$ of landslide-initiation elevations $fl(elevation)$ to the entire population of elevations $f(elevation)$ (Fig. 3) indicates that areas with elevations between 1200 m and 2800 m, where the ratio is greater than one, were preferentially susceptible to landslides during Hurricane Mitch. Available rainfall data indicate that these areas were probably preferentially susceptible to landslides because they received greater amounts of rainfall than areas at lower elevations. Although there were only

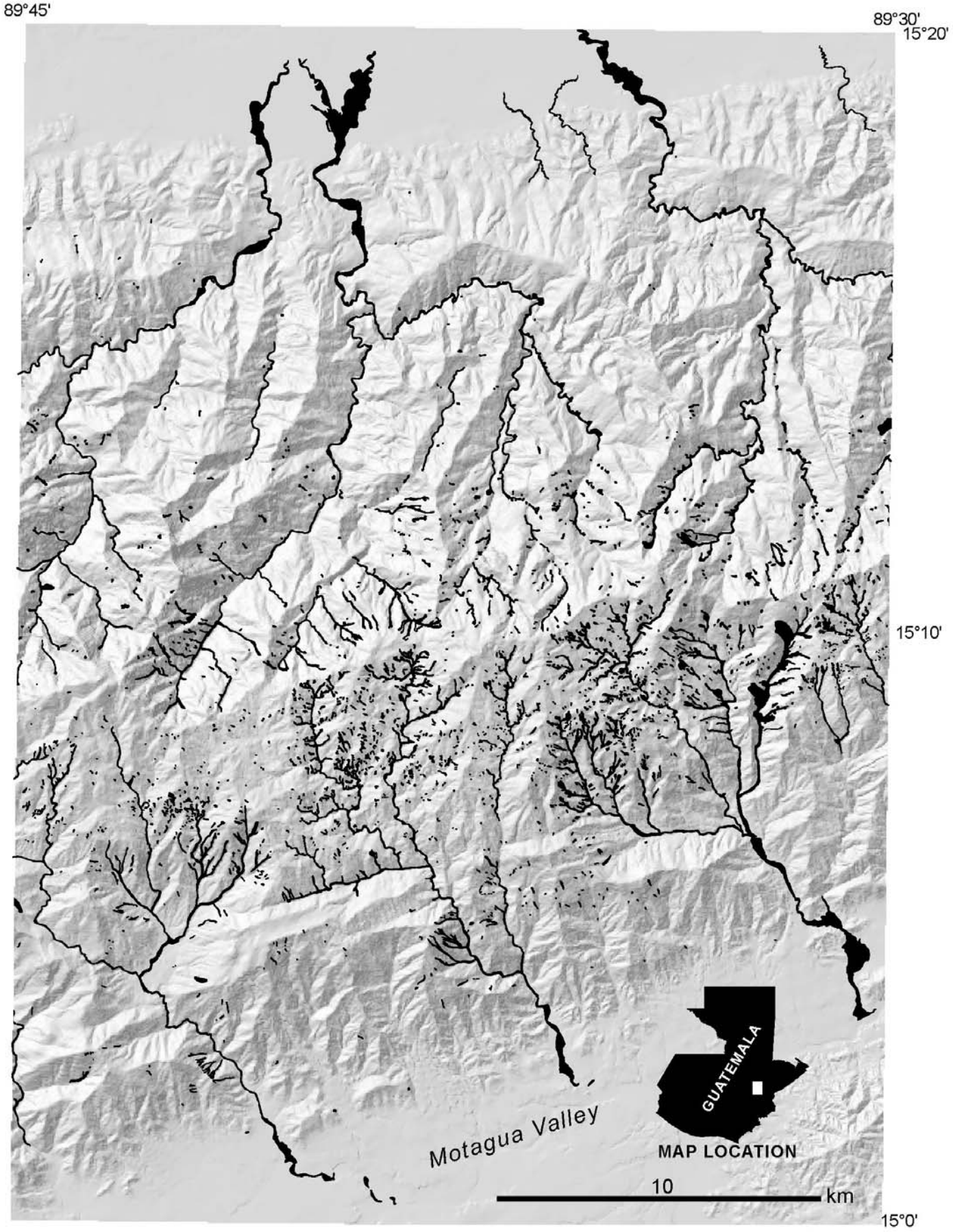

Figure 1. Map showing location of study area and landslides triggered by Hurricane Mitch within the Río Hondo (southern half of the map) and Pueblo Viejo (northern half of the map) topographic map quadrangles.

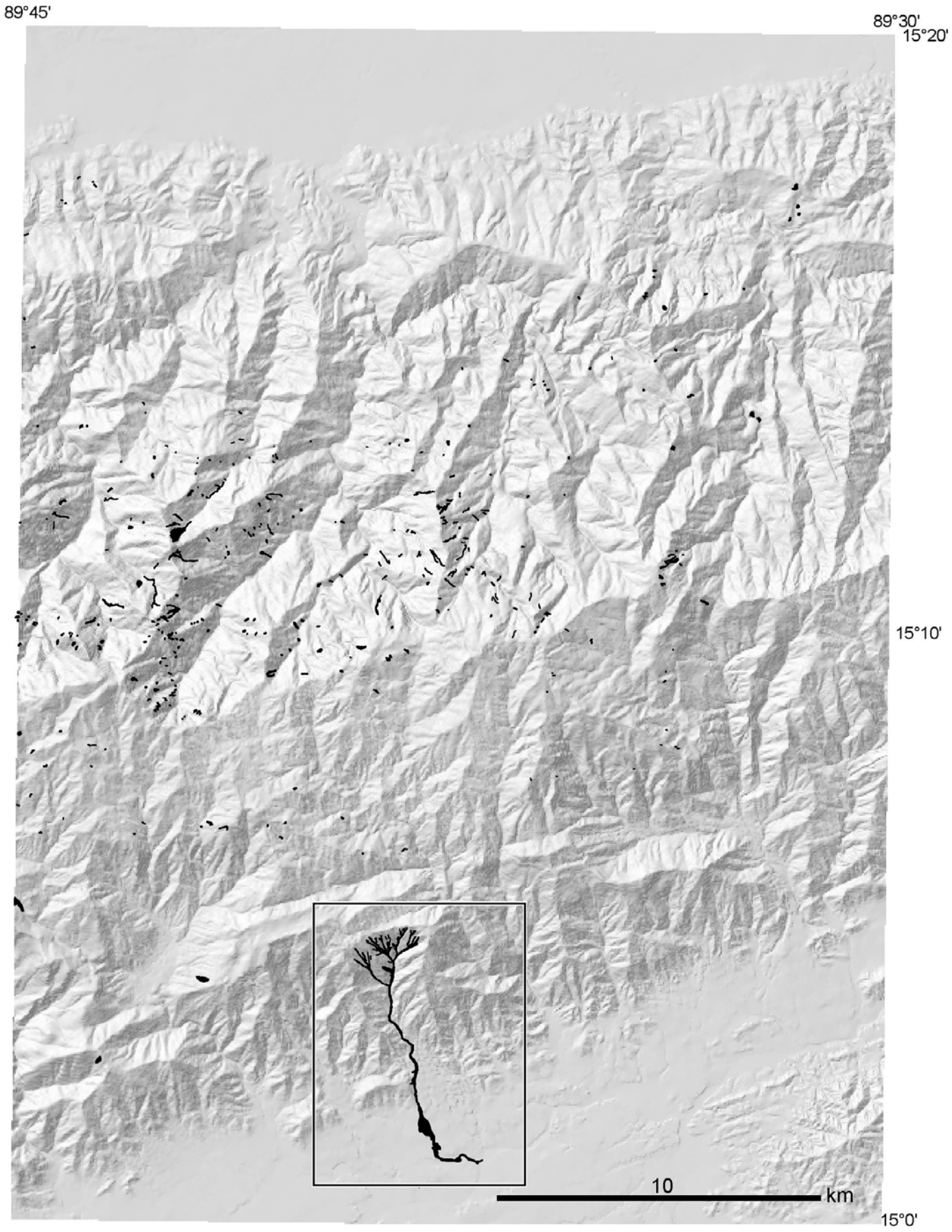

Figure 2. Map showing pre- (outside box) and post-Mitch (inside box) landslides within the study area.

two gages operating in the study area during Mitch, data from these gages show that about twice as much rain fell at 1780 m as at 250 m. Differences in the density and species of vegetation (high density, cloud-forest species at higher elevations; low-density, arid species at lower elevations) suggest that long-term patterns (e.g., annual) of rainfall are also controlled by elevation. However, the abundance of landslides at higher elevations (Figs. 1, 3) indicates that Mitch rainfall at higher elevations was exceptional for the region.

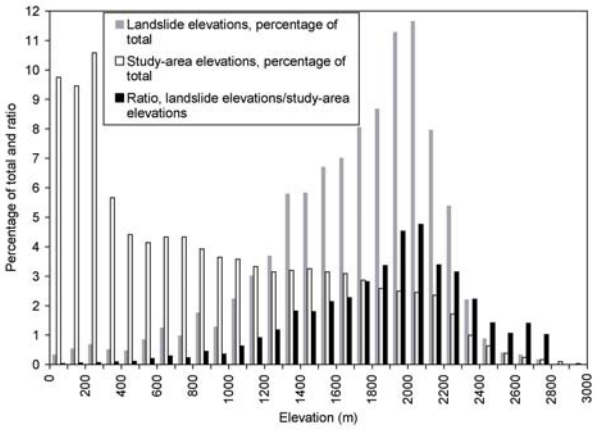

Figure 3. Histograms of elevations measured from the 10-m DEM. Number of 10-m cells in the study area is about 10 million. Number of Mitch landslides is 2951. The ratio *R*(*elevation*) was computed by dividing the percentage of landslide elevations *fl*(*elevation*)by the percentage of study-area elevations *f*(*elevation*)for each histogram bin.

3.2 Analysis of Slope Angle

About 96 percent of the landslides initiated from slopes between 16° and 44° (Fig. 4). When landslide frequency is tabulated in 2° slope-angle bins, the highest percentage of landslides (about 11 percent of the total) initiated between 26° and 28°. The entire population of slope angles at 10-m DEM cells in the two quadrangles ranges up to 75°. The highest percentage of these slope angles (about 11 percent of the total) is between 2° and 4° (Fig. 4). The ratio *R*(*slope angle*) of landslide-initiation slope angles *fl*(*slope angle*) to the entire population of slope angles *f*(*slope angle*) (Fig. 4) indicates that areas with slope angles between 18° and 42°, where the ratio is greater than one, were preferentially susceptible to landslides during Mitch. There is little positive correlation between the calculated ratio and slope angle above 18º. Rather our data seem to indicate that all areas with slope angles above about 18° were roughly equally susceptible to landslides during Mitch. This observation, however, does not take into account the distribution of slope angles with respect to elevation, which we use as a proxy for rainfall.

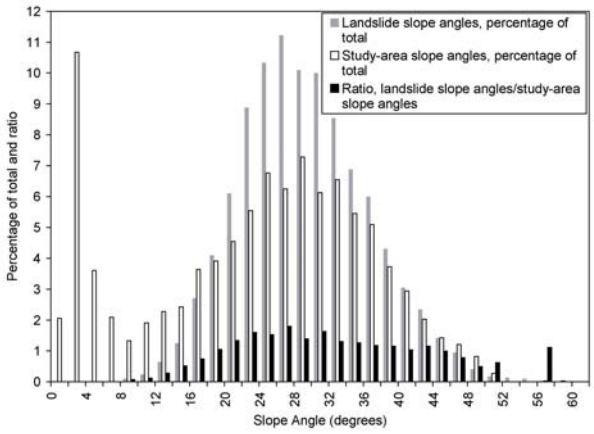

Figure 4. Histograms of slope angles measured from the slope-angle grid. The ratio *R*(*slope angle*) was computed by dividing the percentage of landslide slope angles *fl*(*slope angle*) by the percentage of study-area slope angles *f*(*slope angle*) for each histogram bin.

3.3 Creation of the susceptibility map

An analysis of landslide incidence with respect to both slope angle and elevation, a proxy for rainfall, provides some additional insight into landslide susceptibility and allows for the creation of a relative susceptibility map that incorporates the two parameters. The first step in creating the susceptibility map was to extract two digital files (in a two column format) from the DEM, one containing elevations and slope angles at each landslide-initiation cell, and one containing elevations and slope angles at DEM cells within the study area (Fig. 5a). We used a random sample of cells within the study area, as opposed to the entire population of cells, because the entire population consisted of about 10 million cells and would have been cumbersome to analyze. We used moving count-circle software developed by Savage et al. (2001) to count the frequencies of elevation and slope-angle pairs in these two files. This software established a grid in the slope-angle (x) and elevation (y) plane and counted the number of cells with specific x and y values falling within the neighborhood of each grid location (Fig. 5b). We normalized the axes to make them dimensionless and to create the same number of increments (60, Fig. 5b) in both coordinate directions. The radius of the count circle was one increment (Fig. 5b). Next, the count at each grid location was normalized to a percentage of the total number of landslide cells or randomly sampled population cells (for the landslide-initiation grid *fl*(*slope angle*, *elevation*) and study-area grid *f*(*slope angle*, *elevation*), respectively, Fig. 5c). A contoured version of the two grids is shown in Figure 6a. The ratio of these two grids, computed by dividing the landslide-initiation percentage grid by the study-area percentage grid, provides a ratio grid *R*(*slope angle*, *elevation*)

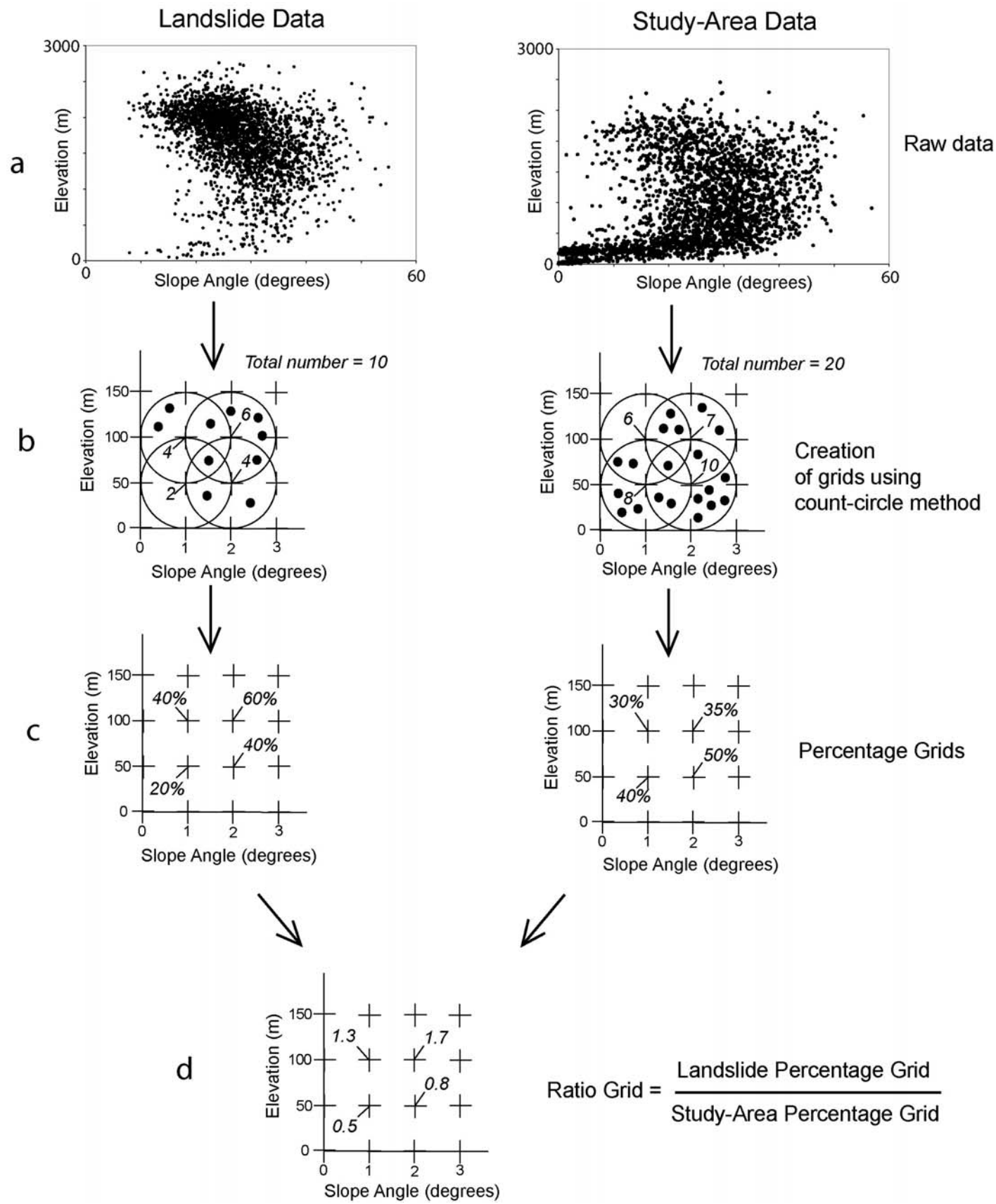

Figure 5. Flow diagram showing how the susceptibility ratio grid *R*(*slope angle, elevation*) was created. a) scatter diagrams of raw data. b) creation of grids and counting using a moving count-circle. c) percentage grid created from the count divided by the total number of points. d) ratio grid *R*(*slope angle, elevation*) created from the two percentage grids.

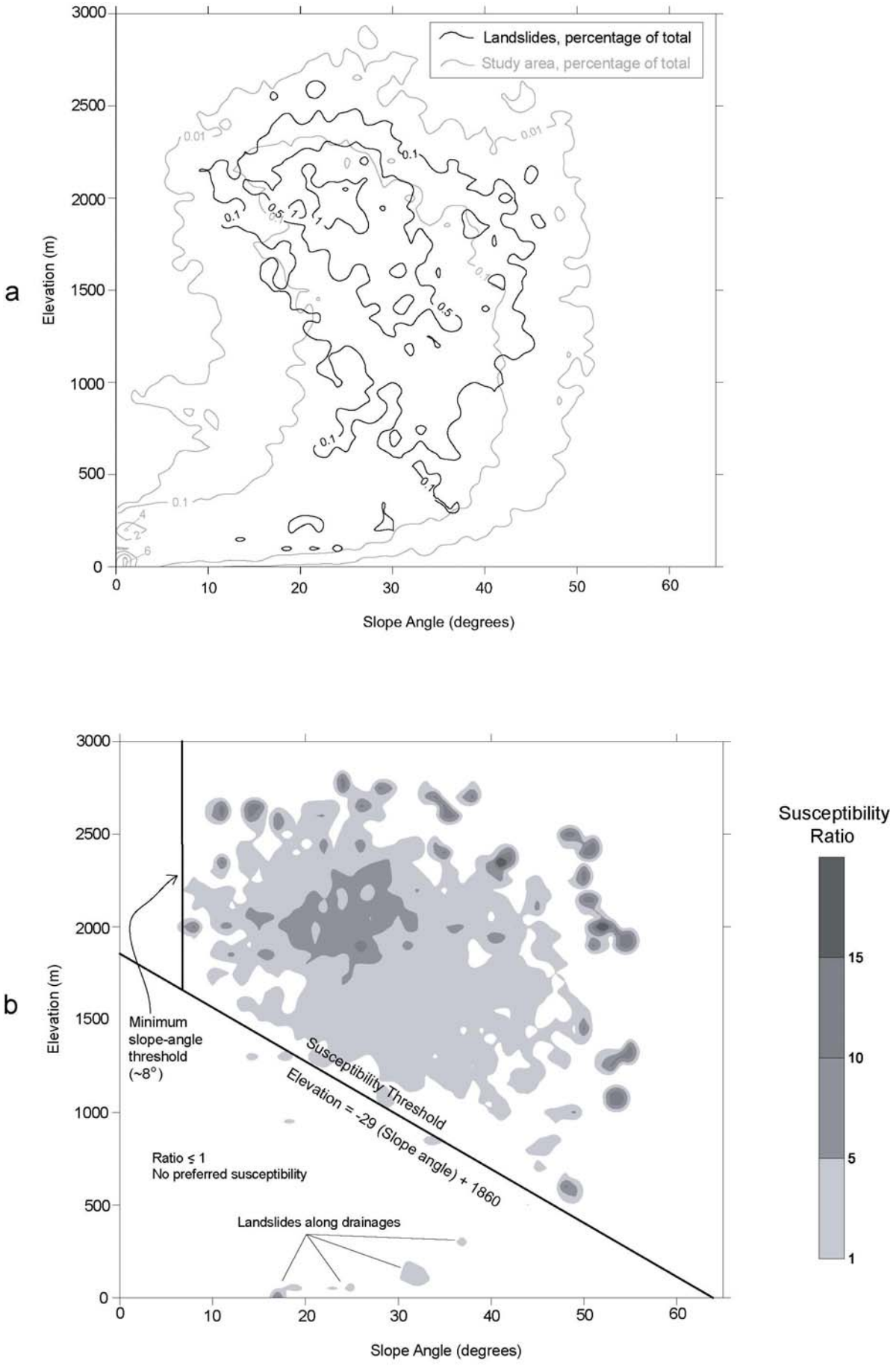

Figure 6. Diagram showing grids for landslide-initiation locations and a random sample of study-area locations. a) Contoured versions of each percentage grid. b) Ratio of the two grids *R*(*slope angle, elevation*) computed by dividing the landslide-percentage grid *fl*(*slope angle, elevation*) by the study-area percentage grid *f*(*slope angle, elevation*). Areas with ratios greater than one are preferentially susceptible to landslide occurrence, whereas areas with ratios less than or equal to one have no preferred susceptibility.

(Figs. 5d, 6b). The ratio grid shows relative levels of susceptibility during and shortly after rainfall from Hurricane Mitch. For example, a ratio of 5 indicates that the area was five times more susceptible than an area with a ratio of one. The ratio grid shows a distinct cluster of preferred susceptibility during Mitch (Fig. 6b). A straight line with the equation $y = -29x + 1860$, where y is elevation and x is slope angle can be fit to the lower bound of the cluster. This line defines a susceptibility threshold, that is, elevations above the line had a preferred susceptibility to landslides during Mitch, and those below the line had no preferred susceptibility. The left edge of the cluster defines a minimum slope-angle threshold, that is, slope angles to the left of the threshold (≤ 8°) had no preferred susceptibility, whereas slope angles to the right of the threshold (>8º) were preferentially susceptible. The susceptibility threshold makes intuitive sense because it indicates that as the minimum elevation of susceptibility decreased, minimum slope angle increased. That is, because elevation was a proxy for Mitch rainfall, the amount of rain (elevation) required to make steep slopes fail was less than that required to make shallow slopes fail. To convert the ratio grid *R*(*slope angle, elevation*) into a susceptibility map, software was developed that used the ratio grid as a lookup table to assign ratio values to map locations based on values read from elevation and slope-angle grids. For example, at every location where slope angle was 30º and elevation was 2000 m, the software assigned a ratio value of 5. The resulting landslide susceptibility map is shown in Figure 7.

4 DISCUSSION

In general, the landslide susceptibility map (Fig. 7) shows that susceptibility (i.e., the ratio value *R*(*slope angle, elevation*)) during Hurricane Mitch increased with elevation, provided that slope angles were greater than about 8º. An exception to this statement is that areas with the highest elevations, as well as with adequate slope angles (the center left side of Fig. 7), were not susceptible to landslides during Mitch. A limitation of the susceptibility map is that it does not show specific landslide travel paths. The inclusion of drainage channels on the susceptibility map (as done in Figure 7) is useful for delineating probable travel paths downslope from susceptible initiation areas.

The effectiveness of the map can be evaluated by examining two percentages, the percentage of landslide-initiation locations that fall within areas of preferred susceptibility (ratios > 1), and the percentage of the study area that has no preferred susceptibility (ratios ≤ 1). A primary goal of susceptibility mapping is to maximize both values. Maps from elevation and slope angle alone (which are not shown because of space restrictions) do the best job of maximizing the percentage of landslide-initiation locations included in susceptible areas (87 and 86 percent, respectively), but do less well in maximizing areas of no preferred susceptibility (66 and 36 percent, respectively). The susceptibility map created from a combination of elevation and slope angle (Fig. 7) provides an optimal solution, with 80 percent landslide locations included in the susceptible zone and 71 percent of the area having no preferred susceptibility.

The effectiveness of the map as a prediction tool can be evaluated using the locations of pre- and post-Mitch landslides (Fig. 2). Seventy-five percent of the pre-Mitch landslides, and 90 percent of the post-Mitch landslides, fall within areas of preferred susceptibility. These high percentages suggest that the positive correlation between elevation and rainfall that was observed during Mitch also applies to more commonly occurring rainstorms, and that the susceptibility map is applicable for predicting landslide locations during these storms.

The susceptibility map was produced using two topographic parameters, but a map could be produced from multiple parameters. In practice, a count sphere (instead of a two-dimensional circle) would easily allow for the use of three parameters. For more than 3 parameters, a more sophisticated binning tool would be required.

The method could be used with multiple inventories from the same area to produce a composite susceptibility map. We expect that the accuracy of such a susceptibility map as a predictive tool will be positively correlated with the number of landslide inventories used to create the map. That is, accuracy would increase as the number of inventories increases. Additionally, the method could provide a powerful tool to compare and contrast susceptibility from similar or different (e.g., earthquake vs. precipitation) triggers in the same geographic area.

5 CONCLUSIONS

Results from this study lead us to make the following conclusions.

(1) The ratio and count-circle approach described in this paper provides an effective way to discriminate and combine topographic parameters to estimate landslide susceptibility, but is limited to areas where landslide inventory and DEM data are available.

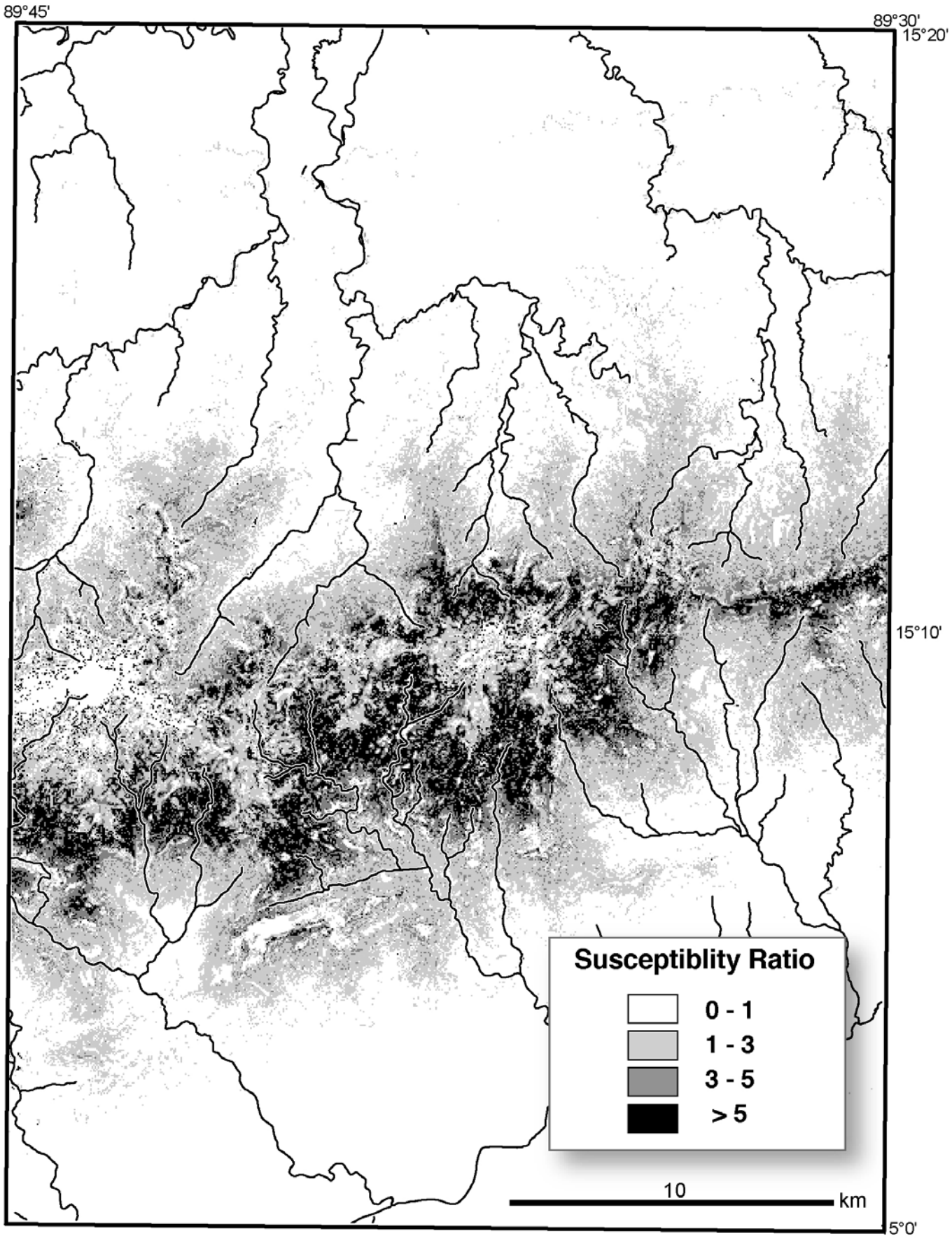

Figure 7. Landslide susceptibility map produced from the ratio grid shown in figure 6b. Areas with ratios greater than one are preferentially susceptible to landslide occurrence, whereas areas with ratios less than or equal to one have no preferred susceptibility. Drainage channels are from 1:50,000 scale topographic maps. Some of these channels were debris-flow travel paths during Hurricane Mitch (see Fig. 1).

(2) In our Guatemala study area, where rainfall accumulation is correlated with elevation, we used the topographic parameters of elevation and slope angle to produce a susceptibility map that shows areas of preferred susceptibility that capture 80 percent of Hurricane Mitch landslide-initiation locations and delineates 71 percent of the study area as having no preferred susceptibility. Seventy-five percent of pre-Mitch landslides, and 90 percent of post-Mitch landslides, also fall within susceptible zones. We expect that similar results could be achieved in other geographic areas where there is a correlation between elevation and rainfall accumulation.

(3) In geographic areas with limited data availability, but a fundamental need for landslide hazard information, a combination of landslide inventory and topographic data can provide an effective estimate of landslide susceptibility.

6 ACKNOWLEDGEMENTS

We thank Dave Lidke and Bill Savage for their critical reviews of this paper.

7 REFERENCES

Bonis, S., Bohnenberger, O.H. & Dengo, G. (compilers) 1970. *Mapa geológico de la Republica de Guatemala*. Instituto Geográfico Nacional. scale 1:500,000.

Bucknam, R.C., Coe, J.A., Chavarría, M.M., Godt, J.W., Tarr, A.C., Bradley, L., Rafferty, S.A., Hancock, D., Dart, R.L. & Johnson, M.L. 2001. *Landslides triggered by Hurricane Mitch in Guatemala—Inventory and Discussion*. U.S. Geological Survey Open File Report 01-443. 39 p. 23 plates at 1:50,000 scale. http://greenwood.cr.usgs.gov/pub/open-file-reports/ofr-01-0443/

Chung, C.F. & Fabbri, A.G. 1999. Probabilistic prediction models for landslide hazard mapping. *Photogrammetric Engineering and Remote Sensing* 65: 1389-1399.

Coe, J.A. & Godt, J.W.. 2001. *Debris flows triggered by the El Niño rainstorm of February 2-3, 1998, Walpert Ridge and vicinity, Alameda County, California*. U.S. Geological Survey Miscellaneous Field Studies Map MF-2384. 3 plates at 1:24,000 scale. http://geology.cr.usgs.gov/pub/mf-maps/mf-2384/

Espinosa, A.F. 1976. *The Guatemalan earthquake of February 4, 1976, A preliminary report*. U.S. Geological Survey Professional Paper 1002. 90 p.

Fabbri, A.G., Chung, C.F., Cendrero, A. & Remondo, J. 2003. Is prediction of future landslides possible with a GIS? *Natural Hazards* 30: 487-499.

Guzzetti, F., Carrara, A., Cardinali, M. & Reichenbach, P. 1999. Landslide hazard evaluation: a review of current techniques and their application in a multi-scale study, Central Italy. *Geomorphology* 31: 181-216.

Jibson, R.W., Harp, E.L., & Michael, J.A. 2000. A method for producing digital probabilistic seismic landslide hazard maps. *Engineering Geology* 58: 271-289.

Lee S., Chwae, U. & Min, K. 2002. Landslide susceptibility mapping by correlation between topography and geological structure: the Janghung area, Korea. *Geomorphology* 46: 149-162.

Lineback, G.M., Marcus, W.A., Aspinall, R. & Custer, S.G. 2001. Assessing landslide potential using GIS, soil wetness modeling and topographic attributes, Payette River, Idaho. *Geomorphology* 37: 149-165.

Lott, N., McCown, S., Graumann, A. & Ross, T. 1999. *Mitch: the deadliest Atlantic hurricane since 1780*. http://lwf.ncdc.noaa.gov/oa/reports/mitch/mitch.html.

Montgomery, D.R. & Dietrich W.E. 1994. A physically based model for the topographic control on shallow landsliding. *Water Resources Research* 30: 1153-1171.

Newcomb, W.E. (compiler) 1978. *Geologic map of Guatemala, Río Hondo: Guatemala*. Instituto Geográfico Nacional. Mapa Geológico de Guatemala. Hoja 2261 II G. scale 1:50,000.

Pallàs, R., Vilaplana, J.M., Guinau, M, Falgàs, Alemany, X. & Muñoz, A. in press. A pragmatic approach to debris flow hazard mapping in areas affected by Hurricane Mitch: example from NW Nicaragua. *Engineering Geology*.

Santacana, N., Baeza, B., Corominas, J., De Paz, A. & Marturiá, J. 2003. A GIS-based multivariate statistical analysis for shallow landslide susceptibility mapping in La Pobla de Lillet area (Eastern Pyrenees, Spain). *Natural Hazards* 30: 281-295.

Savage, W.Z., Coe, J.A. & Sweeney, R. E. 2001. *PTCOUNT -- A Fortran-77 computer program to calculate the areal distribution of mapped data points using count-circle methodology*. U.S. Geological Survey Open File Report 01-0002. 10 p. http://greenwood.cr.usgs.gov/pub/open-file-reports/ofr-01-0002/

Savage, W.Z., Godt, J.W. & Baum, R.L. 2003. A model for spatially and temporally distributed shallow landslide initiation by rainfall infiltration. In D. Rickenmann & C. Chen (eds), *Debris flow hazards mitigation: mechanics, prediction, and assessment*: 179-187. Rotterdam: Millpress.

Savage, W.Z., Godt, J.W. & Baum, R.L. this volume. Modeling time-dependent areal slope stability.

Soeters, R. & van Westen, C.J. 1996. Slope instability recognition, analysis, and zonation. In A.K. Turner & R.L. Schuster (eds), *Landslides–Investigation and Mitigation: 129-177*. Washington, D.C.: National Academy Press. National Research Council. Transportation Research Board Special Report 247.

Tobisch, M.K. 1986. *Part I, late Cenozoic geology of the central Motagua Valley, Guatemala - Part II, uplift rates, deformation and neotectonics of Holocene marine terraces from Point Delgado to Cape Mendocino, California*: 364. Santa Cruz: University of California. Ph.D. thesis.

Wieczorek, G.F., Harp, E.L., Mark, R.K. & Bhattacharyya, A.K.. 1988. Debris flows and other landslides in San Mateo, Santa Cruz, Contra Costa, Alameda, Napa, Solano, Sonoma, Lake, and Yolo Counties, and factors influencing debris-flow distribution. In S.D. Ellen & G.F. Wieczorek (eds), *Landslides, floods, and marine effects of the storm of January 3-5, 1982, in the San Francisco Bay region, California*: 133-162. U.S. Geological Survey Professional Paper 1434.